

We are IntechOpen, the world's leading publisher of Open Access books Built by scientists, for scientists

4,800

Open access books available

122,000

International authors and editors

135M

Downloads

Our authors are among the

154

Countries delivered to

TOP 1%

most cited scientists

12.2%

Contributors from top 500 universities

**WEB OF SCIENCE™**Selection of our books indexed in the Book Citation Index
in Web of Science™ Core Collection (BKCI)

Interested in publishing with us? Contact book.department@intechopen.com

Numbers displayed above are based on latest data collected.

For more information visit www.intechopen.com

Topological Analysis of Tokyo Metropolitan Railway System

Takeshi Ozeki

*Faculty of Science and Technology, Sophia University
Japan*

1. Introduction

1.1 Railway system reflects the real world

Leading concept of the topological analysis of railway network systems is based on the fact that the topology of railway networks reflects the real world. It is believed because strong mutual interactions between railway systems and real worlds continue through longer periods of their growth: An eventual growth in a regional economy due to opening such a new shopping plaza may require extension of a railway system, verves, a scheduled extension of a railway may result in a growth in regional economy due to rapid increase in town population, for instance. In this way, the growth of railway system and regional activity affects their growth mutually. In context, the railway system topology reflects the real world: In other words, they “entangle” each other.

This leading concept agrees with that of Brin and Page, co-founders of Google: they reported, in their first paper on “Google” (Page and et al, 1990), that it was a great surprise the PageRank is obtained purely mechanically from the topology of Web page links. Their surprise is the discovery of the fact that the network is entangled with real world. The “Google” approximates a Web surfer as a random walker in Markov process and combines the dominant eigenvector of Markov process with a list of coincidence for a inquiry as the PageRank (Langville-Mayer, 2006)

This leading concept grows up as a mathematical platform using multimodal non-linear Markov process approximation so that it is applied to analyse Tokyo Metropolitan Railway System.

It is no doubt that there have been established platforms to analyse the dynamics of railway network systems based on growing supercomputer power. On contrary, our platform can be said as providing abstractive viewpoint based only on network topology so that it is expected to illustrate different new worlds for the railway system engineers.

1.2 Family network approximation: Rosary network

Network topologies have been discussed as scale free networks mainly in a field of complex systems from the end of the previous century. The scale free network science is expected to provide potential methods to analyse various network characteristics of complex systems.

However, there is no network model suitable for analysing railway systems. Then, the rosary network in series of family the network was proposed as suitable one for railway system networks as shown in Fig.1.1 (Ozeki, 2006).

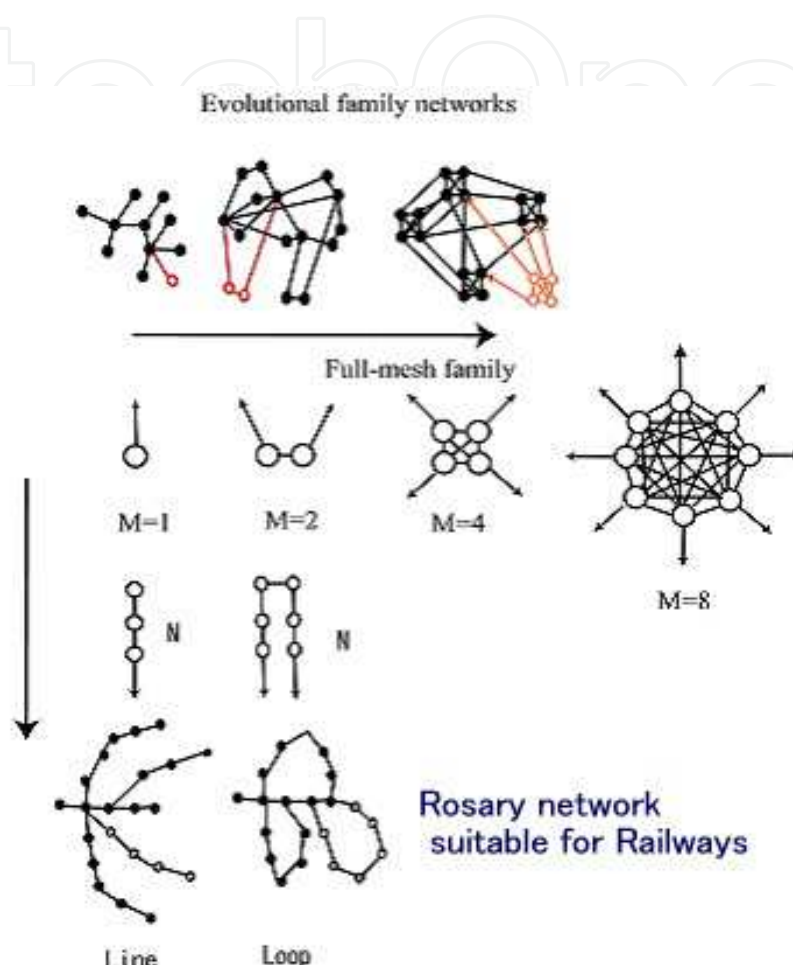


Fig. 1.1. Family network Series including Rosary Networks

Historical flows of complex systems are very interesting competitions between abstraction and computation: Origin of complex systems was introduced by Prigogine based on coupled nonlinear differential equations and sophisticated chemical experiments (Prigogine, 1981). It was followed by distributed agent model supported by rapidly growing computational power. However, for analysis of huge network systems the distributed agent model was suffered by computational complexity explosion in 1990'. Then, abstractive approaches such as scale free networks become to share exploring complex network systems. Topological analysis of railway network is backed by these historical flows.

The Watts-Strogatz's small world evolves from regular lattice networks to the Erdos-Renyi's random networks (Erdos, 1960) by random rewiring links with a given probability (Watts, 1998). The Watts-Strogatz's small world having fixed number of nodes is discussed as a static network. On the other hand, the scale-free network of Barabasi-Albert (BA model) introduces the concept of growing networks with preferential attachment (Barabasi, 1999). One of characterizations of networks is given by the connectivity distribution of $P(k)$, which is the probability that a node has k degrees (or, number of links). In the scale free networks based on BA model, the connectivity distribution follows the power law, in which $P(k)$ is approximated to $k^{-\gamma}$, having the exponent $\gamma=3$. The real world complex networks are analysed to find various scale free networks having various exponents, which are covered in references (Newman, 2006). For an example, it is well known that social infrastructure networks, such as power grids, as egalitarian networks, follow the power law with exponent 4 (Barabasi, 2002). There were many trials reported to generate models with larger exponents for fitting these real-world networks (Newman, 2006): Dorogovtsev *et al* (Dorogovtsev, 2000) modified the preferential attachment probability and derived the exact asymptotic solution of the connectivity distribution showing the wide range of exponents $\gamma = a + 2$, where a is the attractiveness. However, there was no network generation model suitable for analysing railway systems.

In context, "the evolutionary family networks" generated by "a group entry growth mechanism" with the preferential attachment was proposed in ICCS2006 (Ozeki, 2006): growth mechanism employed is group entry having constituent family connected in full-mesh, line and loop. This is suitable to simulate the railway system: as shown in Fig.1.1, a graph in the bottom looks like a railway system; We call it "Rosary network approximation" that will be discussed in the case of Tokyo metropolitan railway system in section 2. Various characteristics will be analysed based on the Multi-modal Markov transition approximation in section 3.

1.3 Birds with a feather flock together

We point out that nonlinear effects are inevitable in the passenger flow analysis. Since the Google is an infrastructure in daily life same as railway system, we refer the Google: the Google is characterized by a single dominant mode: In linear Markov transition, the asymptotic state is always the dominant mode. However, a Japanese adage: "people wish to get together to the place where people get together" or "Birds with a feather flock together" is important in real world to determine such PageRanking. The Google assumes such tendency is reflected in the page link network. Here, we point out it is not always sufficient, and demonstrate a Markov engine with the third-order nonlinear interaction reflecting such tendency to retrieve a real world, correctly.

We demonstrated the new engine to retrieve *the largest three stations* in respect of number of passengers in Tokyo Metropolitan Railway Network, in section 4.

1.4 TSUBO: Impulse response of network

We discuss "key stations of railway network dynamics" by analogy with "Tsubo in Shiatsu".

In Japan, “Shiatsu” is a popular therapy by pressing “shiatsu point” to enhance the body’s natural healing ability and prevent the progression of disease. Shiatsu points are called “Tsubo”, in Japanese. Their locations and effects are based on understanding of modern anatomy and physiology. The concept of “Tsubo” has been used as a strategy in re-activation of an old city, such as Padova, Italy (Horiike, 2000). He calls it “the Point Stimulus”. The “Point Stimulus Response” corresponds to the impulse response of the network system, that is, the temporal state variation in the Markov transition to the delta-function with negative sign of initial state. We can evaluate the node activity by its response to the point stimulus.

We will discuss “Tsubo” of Tokyo metropolitan railway system in session 5.

2. Scale free characteristics of railway network

We show here a large railway system, such as Tokyo metropolitan railway system, that indicates characteristics of scale free networks: “station” corresponds to “node”, and “track” to “link”. This section is based on our paper presented in ICCS 2006. (Ozeki 2006)

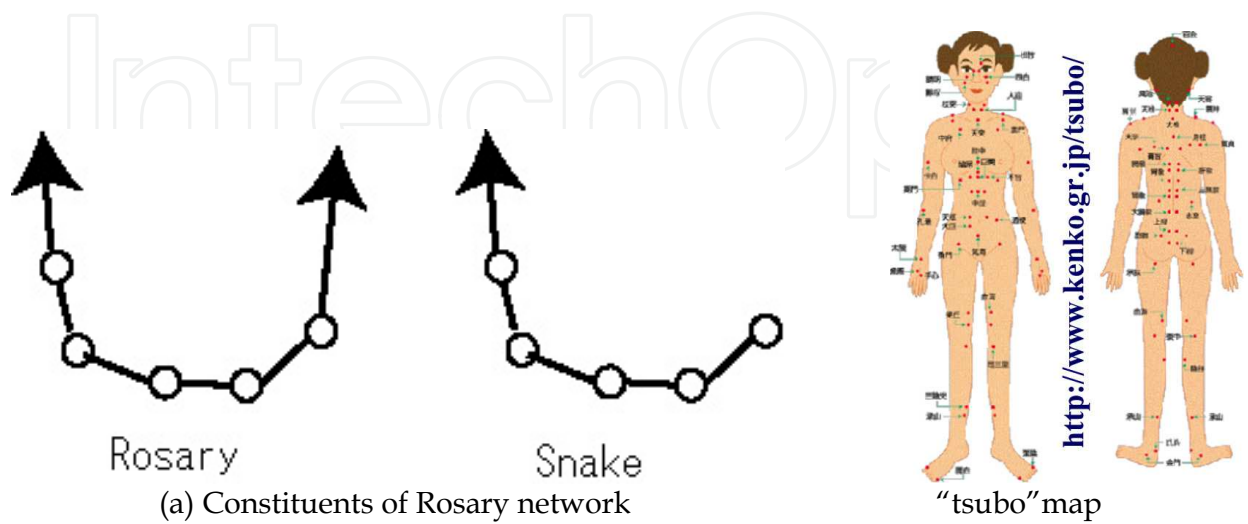
2.1 Growth mechanism of Rosary

A growth step of a railway network is modelled as illustrated in Fig.2.1 (a): a rosary that consists of M stations connected in a shape like a rosary is added to an old railway network. There are two cases of its constituent: one is like a rosary having two jointing links as shown in Fig.2.1 (a) left, the other is like a snake having one jointing link as shown in Fig.2.1-right. Fig.2.1 (b) is a rosary network generated this growth mechanism: assuming the fraction of snakes in constituent groups to be 10% and growth step 11 for convenience to grapes its perspective. This topology is drawn by a free-software: Cytoscape (<http://www.cytoscape.org/download.html>). The initial constituent is a group #0~#8 and the total number of stations is 65. The degree distribution is illustrated in Fig.2.1(c) (the “degree” denotes the number of links of a node). The degree distribution follows the power law with exponent of -4 as shown in Fig.2.1 (c).

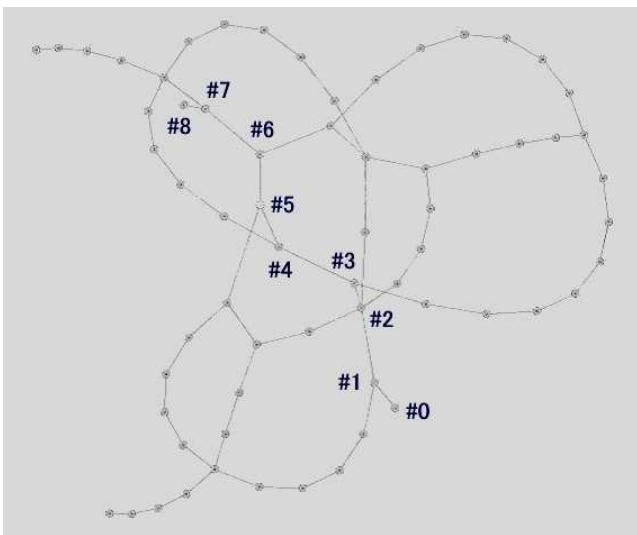
2.2 Multimodal analysis of Rosary network

Before analysing Tokyo Metropolitan Railway System, it seems better to analyse this small rosary network. We assume a passenger in the rosary railway network as “a random walker”, that is equivalent to multimodal Markov transition approximation (refer Appendix 1). The dominant mode of the multimodal Markov transition corresponds to the stationary state of passenger distribution that is illustrated in Fig.2.2 (c). The eigenvector of dominant mode has a peak at station #2, and mountains in the dominant eigenvector are illustrated in Fig.4.3 (a): the original station group #0~#8 corresponds to the first mountain in the figure, and the followings are illustrated in blue rosaries. The eigenvalue of the rosary network is shown in Fig.2.2 (a): The #64 eigenvalue of 2.773 corresponds to the dominant mode. The 2nd mode has negative largest eigenvalue. The mode competition among these modes in nonlinear multimodal Markov transition is discussed in section 4.

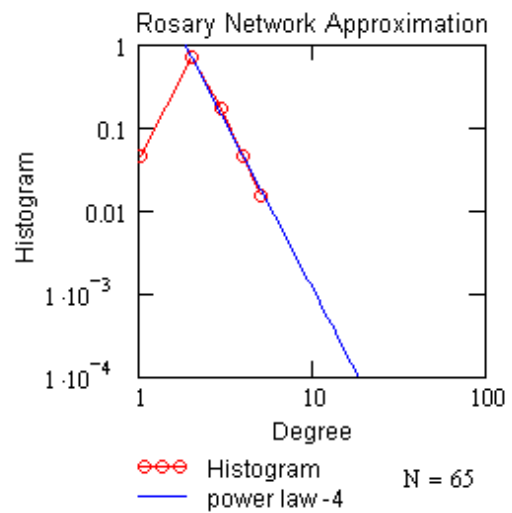
This rosary network has no real world so that it is difficult to show the substructure analysis. Next we discuss a actual rosary network.



Rosary Snake
(a) Constituents of Rosary network



(b) A small rosary network generated.



(c) Power law

Fig. 2.1. Rosary network model suitable for analyzing railway systems.

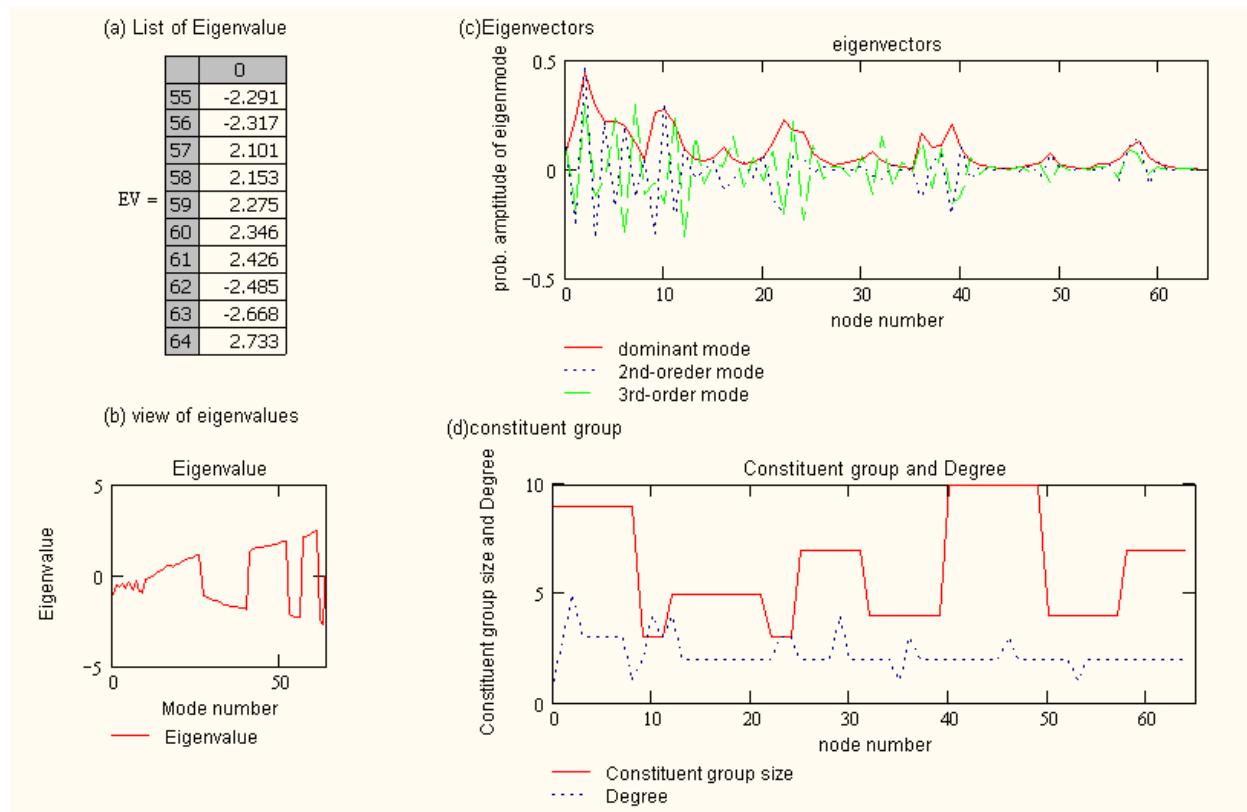


Fig. 2.2. Mode Structure of Rosary Network

3. Analysis of Tokyo metropolitan railway system

Tokyo metropolitan railway system is illustrated in Fig.3.1: (a) denotes the Map of contemporary Tokyo metropolitan railway system (Rail Map of Tokyo Area, 2004) and (b) denotes the map of Edo in 18th century. The central part of Tokyo metropolitan railway is truncated to have the number of total stations of 736. The total number of links is 1762. The number of links is counted topologically: for instance, we count the number of links between Tokyo and Kanda as 1, even though there are three double railways between them. Fig.3.2 (a) depicts degree distribution of a central part of Tokyo Metropolitan Railway System. The excellent fit in degree distribution suggests that the growth mechanism of Tokyo railway system is coincident with the growth mechanism of rosary network. The exponent measured to be 4, which is coincident with those of the small rosary network shown in Fig.2.1 (c) and the power grids of North America (Barabasi, 1999). It is surprising to find that the number of nodes in constituent rosary networks is $M=3$, which is reasonable in the central part of Tokyo with respect to its complexity. A real world railway network is well approximated by our rosary network model.

3.1 Substructures of Tokyo

The main issue is the extraction of an authentic centre (Tokyo, Shinbashi, Shinagawa) and a new metropolitan centre (Shinjuku, Ikebukuro, Shibuya). The later corresponds to the centre and the outskirts of Edo as shown Fig.3.1 (b).



(a) Map of Tokyo Metropolitan Railway System

(b) Map of Edo in Tokugawa Era of 18th Century

(<http://onjweb.com/netbakumaz/edomap/edomap.html>)

Fig. 3.1. Tokyo Metropolitan Railway Network System

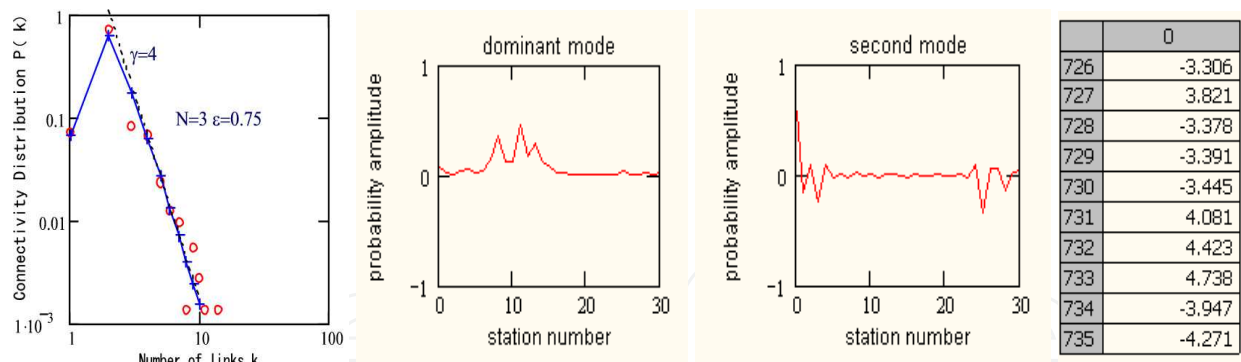
A distorted hexagonal in Fig.3.1 (a) is “*Yamanote Circular Line*” which includes several well-known stations such as Tokyo, Shinbashi, Shinagawa, Shibuya, Shinjuku and Ikebukuro etc.

Fig.3.2 summarizes the mode structures of the network. In a list of eigenvalues illustrated in the right, we focus on the following two modes; the dominant mode #733 with eigenvalue +4.738 has larger probability at *Shinagawa* (station number #8), *Shinbashi* (#11) and *Tokyo* (#13) as shown in middle left panel of Fig.3.2. The constituent stations of the dominant mode are illustrated in Fig.3.1 (a) on the *Yamanote* circular Line.

The second mode #735, having negative largest eigenvalue of -4.271, has larger probability at *Shinjuku* (#0), *Shibuya* (#3) and *Ikebukuro* (#25) as illustrated in middle right panel of Fig.3.2. The constituent stations of mode #735 are also illustrated by *italic character* on the *Yamanote* circular line, in Fig.3.1 (a).

3.2 Orthogonal features of substructures

It is interesting that the dominant mode #733 extracts the central structure of business and government of Metropolitan Tokyo. This area also corresponds to the main structure in Edo metropolitan area. (Tokyo was called *Edo* in 18th century.)



Left: Degree distribution, Middle left: dominant mode; Shinagawa (8), Shinbashi (11), Tokyo (13); Middle right: second mode: Shinjuku (0), Shibuya (3), Ikebukuro(25) Right: List of eigenvalues

Fig. 3.2. Multimodal Analysis of Tokyo Metropolitan Railway System

The bridge of *Nihonbashi* is the original point of national roads including the *Tokaido* (presently *root 1*) in Edo era as shown in Fig.3.1 (b). The main business was blooming along the *Tokaido*, and the political organization was concentrated between the *Edo castle* and the *root 1*. It can be said that the central structure of contemporary Tokyo succeeds the main structure of the *Edo* metropolitan of which population was exceeded one million in 18th century.

On the other hand, the second mode #735 is successor of the *Edo* outskirt villages located in the lower part of Fig.3.1 (b). The eigenmode effectively extracts orthogonal substructures in variety of viewpoints: The dominant mode retrieves the dominant political and business area of present Tokyo metropolitan. The second mode retrieves its most growing area that was the outskirt of *Edo*.

It is suggestive that the probability amplitude of the second mode, illustrated in the middle right panel of Fig.3.2, is positive at *Shinjuku* (station number #0) and negative at *Shibuya* (#3) and *Ikebukuro* (#25). Historically, *Shinjuku*, as the fourth hosting station of *Edo*, leads the others in this outskirt area. It is interesting because this mode profile has strong relations with mode competition in nonlinear Markov transition, as will be discussed in section4.

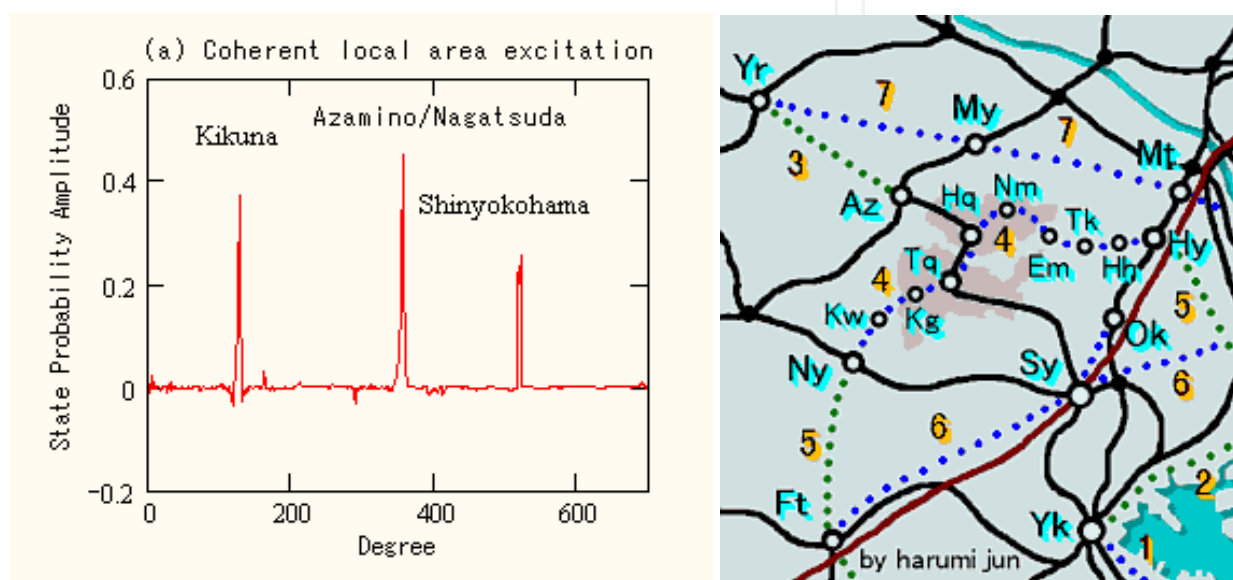
The further interpretation of probability amplitude remains in being unexplored. The data mining technology may be useful to reveal it.

3.3 An interesting eigenmode extracts the *Kohoku* new town project

The study of the *Kohoku* Newtown project is an old graduation thesis of our laboratory, when a different definition of transition matrix was used in Markov transition (Ozeki, 2009). Fig.3.3 (a) denotes the eigenvector of the 200th eigenmode of Tokyo Metropolitan Railway system. It consists of three station groups, named *Azamino / Nagtsuda* group (*Denentoshi* line), *Shin-yokohama* group (*Yokohama* line) and *Kikuna / Ohkurayama* group (*Toyokyu* line). Those are excited coherently and simultaneously in the same phase, as shown in Fig.3.3 (a) A speculation suggests that a zone, encircled by three lines, might be successfully developed as a triangle business park. It is our great surprise to find that “the *Kouhoku* Newtown project” was promoted from 1965 to 1996, exactly in this zone. Fig.3.3 (b) denotes the

railway network map of the project, which shows *Az* for *Azamino* and *Sy* for *Shinyokohama*. *Nagatsuda* marked by *Na* was not recognized as key stations of the Newtown, but presently “*Yokohama city plans*” includes it as the *Yokohama Silicon valley*: It is well known that *Nagatsuda* includes the campus of Tokyo Institute of Technology. This network analysing engine points out the importance of *Nagatsuda* to provide TIT as Stanford University of Silicon valley.

Unfortunately, the network graph, used hitherto, does not include the *Blueline* subway that is one of the main constructions in the *Kohoku* Newtown project. In next, we will discuss the evaluation of *Blueline* project.



(a) The eigenvector #200 coherently excited (b) Kohoku Newtown Project:Kohoku Newtown encircled by the #200 eigen-mode:Sy=Shin-Yokohama, Ok=Ohkura yam, Az=Azamino (<http://www.yk.rim.or.jp/~harujun/ntown/ntftr.html>.)

Fig. 3.3. Eigenvector of *Kohoku* Newtown.

3.4 Evaluation of a new subway project

Here we would like to introduce an interesting application of our network analysis platform: it is a blind evaluation method of network modification project. As introduced in the previous subsection, we try to evaluate the project of “*Blueline*”. The method is the variation of node entropy before and after *Blueline* inauguration, as illustrated in Fig.3.4 (a). The station group with increasing in their node entropy includes *Totsuka* (#94), *Sakuragicho*(#84) and *Kannai* (#85). On the contrary, the station group with decreasing node entropy includes *Hodogaya*(#104) and *Kita-Kamakura*(#106).

We can show a supporting data for this evaluation in Fig.3.4 (b). The number of annual passengers of *Hodogaya* station shows abrupt drop in 1999 when the *Blueline* service was started. This blind-evaluation method presently only provides the variation of passenger flow of modified network, but it seems a powerful tool for network system design in future.

4. Nonlinear phenomena in passenger flow in Tokyo metropolitan railway system

Here we would like to point out that nonlinear phenomena are important in passenger flow analysis. First of all, it should be noted that there are two types of nonlinear phenomena in the third order nonlinear interaction (Agrawal, 1989): one is SFM (Self Phase Modulation) that is equivalent to “Like Button” in Facebook, that is, transition probability to a node having the same opinion increases. (Please refer Appendix to find details including notations.)

This nonlinear Markov transition process is expressed mathematically by the following;

$$(q_i)_{n+1} = \sum_j A_{i,j}(q_j)_n (1 + \gamma(q_i)_n(q_j)_n) \quad (1)$$

In this expression, the nonlinear term $\gamma(q_i)_n(q_j)_n$ might be recognized as “like button”: in case of the state $(q_i)_n$ of node # i having the same sign with $(q_j)_n$, the transition probability from node j to i increases when the nonlinear coefficient γ is positive. In other words, “like button” is a tool to express our personal opinion that controls routing of information in Facebook. It might be reasonable that nonlinear phenomenon in rush hours is recognized as SPM because most of passengers in rush hours have more sharp intention to reach their destinations.

The other is called XPM (Cross Phase Modulation) that is equivalent to “curious bystanders”, that is, the transition probability to a node having many “curious bystanders” increases. It is shown mathematically as following:

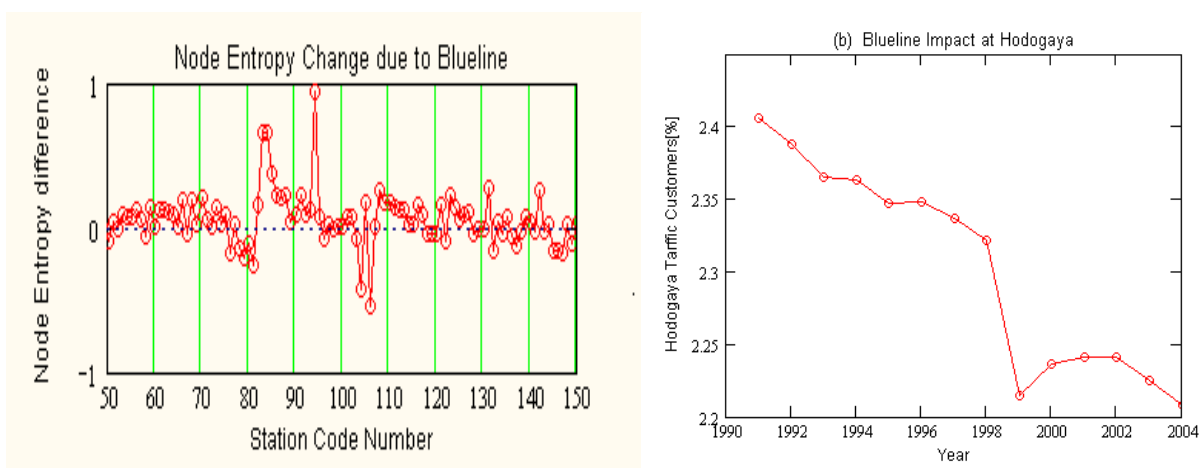


Fig. 3.4. Eigenvector Variation due to the Blueline.:(a) Node Entropy Change due to Blueline. (d) Evolution of Hodogaya Traffic Customers. Operation of Blueline was 1999.

$$(q_i)_{n+1} = \sum_j A_{i,j}(q_j)_n (1 + \gamma \sum_{k,m} A_{i,k} A_{i,m}(q_k)_n (q_m)_n) \quad (2)$$

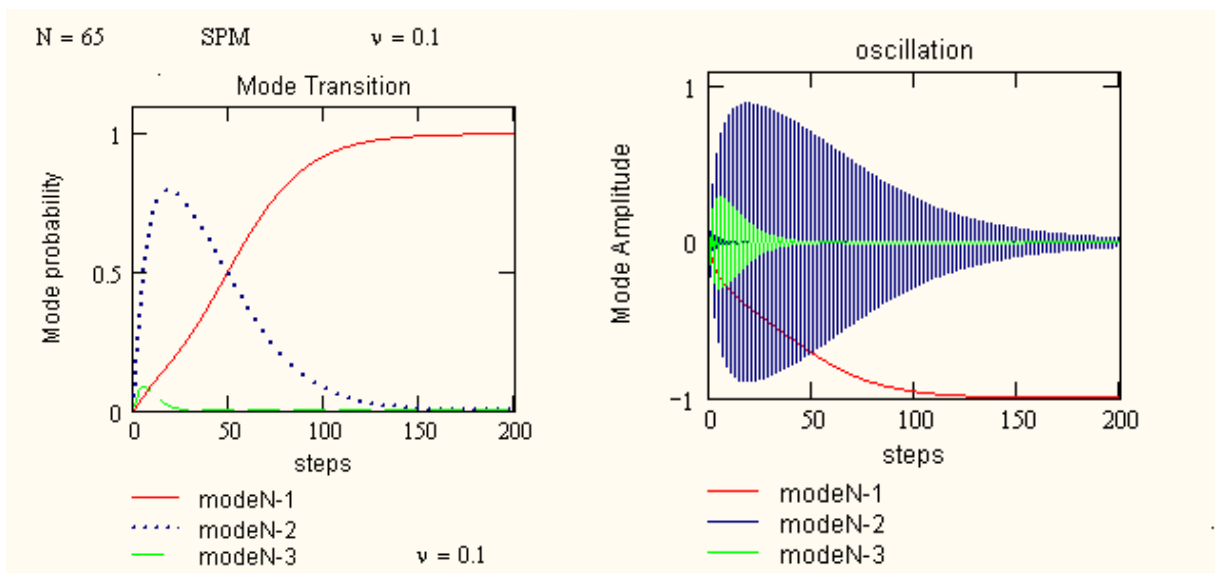
In this expression, the nonlinear term $\sum_{k,m} A_{i,k} A_{i,m}(q_k)_n (q_m)_n$ might be recognized as effect of “curious bystander” because the transition probability from node j to i increases when $(q_k)_n (q_m)_n$ is positive. In other words, XPM expresses “Birds with a feather flock together”.

To make our intention of introduction of SPM and XPM clear, we show their import differences in network dynamics:

Final target is discussion of mode competition between the authentic centre and the new growing metropolitan centre. And the third-order non-linear interaction is inevitable to show that the largest three stations are those in the new growing metropolitan region in Metropolitan Tokyo.

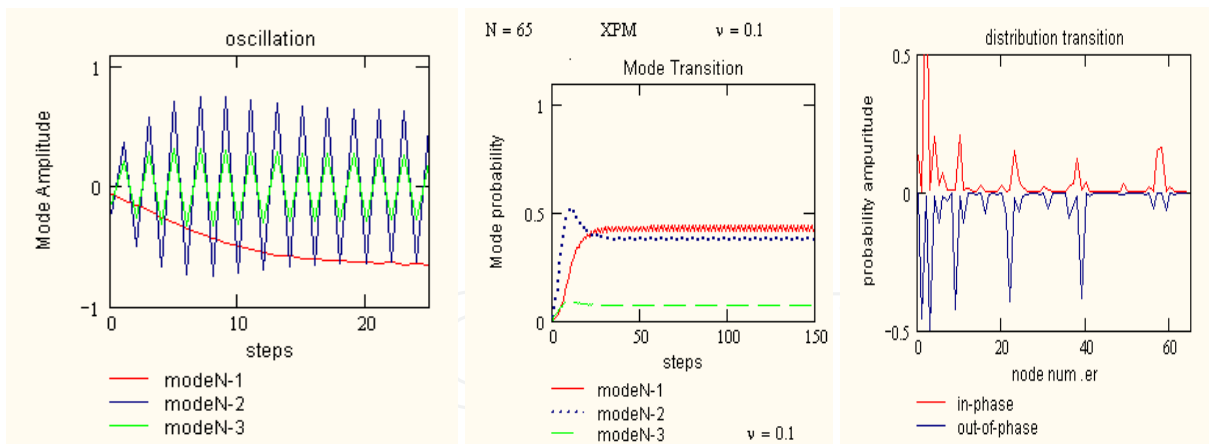
4.1 Emergence of instability

It seems better to introduce “Emergence” in the small rosary network discussed in session 2, before we discuss more complicated Metropolitan Tokyo railway system. Fig.4.1 illustrates the temporal variation of mode probability (the squared mode amplitude) of the nonlinear Markov transition based on Eq.4.1 applied to the small rosary network shown in Fig.2.2. The initial condition is a random distribution of node probability amplitude. SPM with medium $\nu = 0.1$ leads to the dominant mode as the stationary state of the rosary network. It should be noted that the right panel illustrates the temporal variation of the mode amplitudes: The 2nd and 3rd order modes have negative eigenvalues so that the mode amplitudes change their sign at each Markov transition. The dominant mode having positive eigenvalue does not oscillate.



Left diagram indicates mode probability (squared mode amplitudes) and the right diagram denotes the temporal variation of mode amplitudes.

Fig. 4.1. Temporal variation of modes in SPM nonlinear Markov transition from random mode amplitude distribution as initial condition.



The light panel denotes the temporal variation of mode amplitudes. The middle panel denotes the temporal variation of mode probabilities. The right panel denotes two phase of probability amplitude.(the red race inverted in sign for clearness.)

Fig. 4.2. XPM Markov transition of the Rosary network:

On the other hand, Fig.4.2 illustrates the temporal variation of mode amplitudes in the case of XPM nonlinear Markov transition based on Eq.4.2. In this case the rosary network shows “emergence” of a kind of instability: The temporal variation of mode amplitude oscillates as shown in left panel of Fig.4.2. At stationary state, two phases are shown in the right panel of Fig.4.2. At “in-phase” denoted by red, the passengers gather on node #2 and #4 . In “out-of-phase” denoted by blue, the passengers shift to node #1,#3,#9,#22 and #39 coloured by yellow in the map of Fig.4.3 left. Those nodes can be reached from node #2 or #4 within one step. The oscillation is recognized to be sustainable transition between two groups of nodes.

This kind of oscillation has not been reported in real world, yet. One of convenient interpretation is that average of two states is assumed to be observable; that is, we assume the average state corresponds to observable phenomenon in the real world. Fig.4.4 (b) illustrates the average state corresponds to the instability in the XPM Markov transition. Markov transition approximation of a large-scale network has a limitation due to delay time to obtain information of nodes connected to a node, at each transition, so that it might be reasonable to take average of oscillating states, just mentioned above.

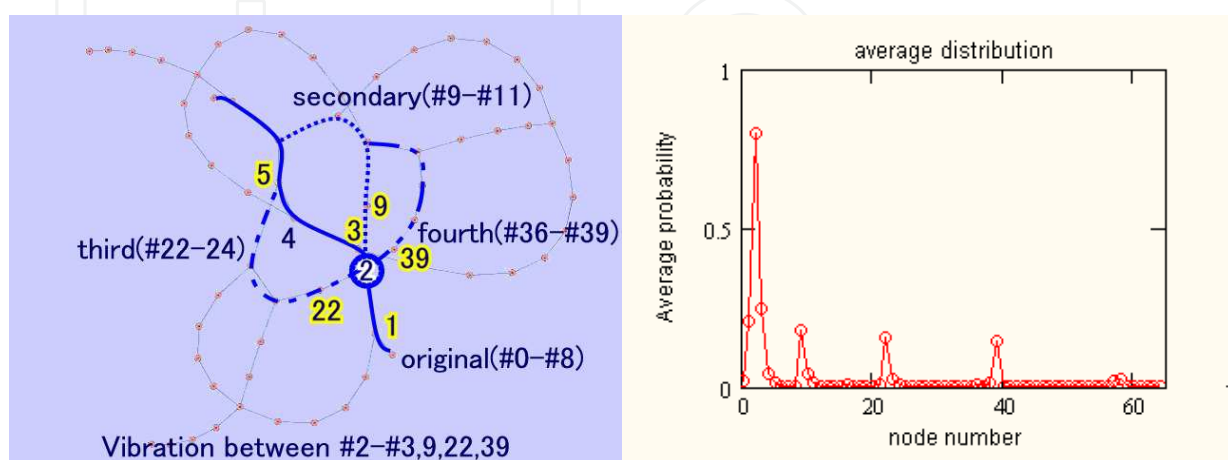


Fig. 4.3. (a) Sustainable oscillation between two groups of nodes (b) Average probability distribution

However, it should be noted that there are many intuitive samples of oscillations in the real world. This oscillation has strong relation with the network controllability and stability. These issues are discussed in Appendix C.

Since available data of the passenger flow analysis in Tokyo railway system are dairy data average over a year, it is reasonable to use the average of probability distribution of Markov transition approximation.

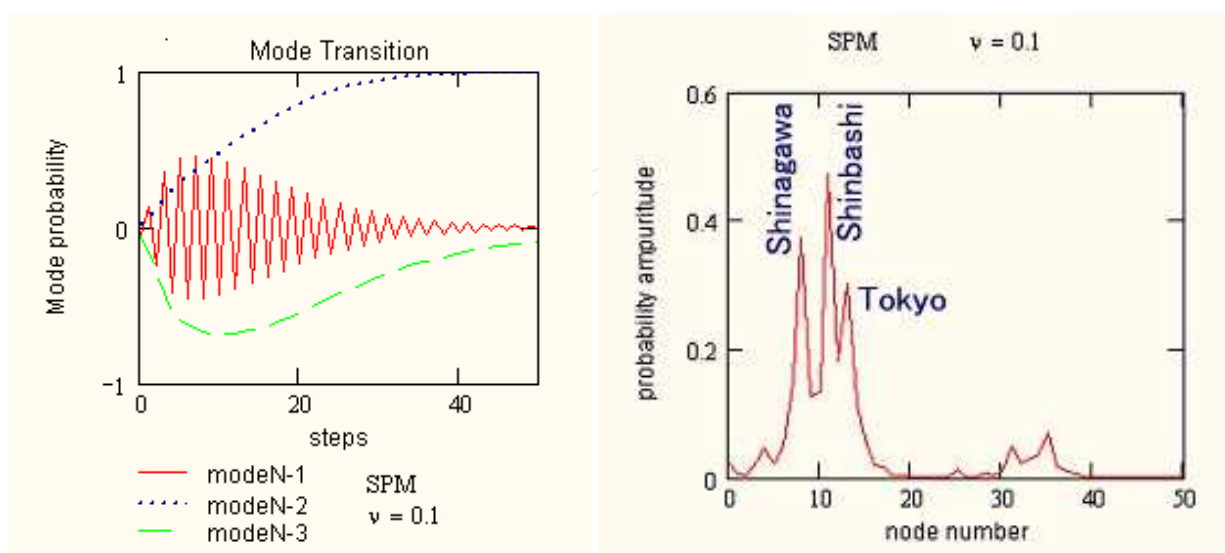
4.2 The largest three stations of Tokyo metropolitan railway

One of the targets is to extract outstanding patterns from huge network system: In linear systems, the dominant mode corresponds to such an outstanding pattern. This understanding coincides with that of the basic Google in which one assumes that passengers in Tokyo railway system can be approximated as random walkers in the linear Markov process. Its stationary state is the dominant mode.

The real world data, however, tell us that the largest three stations, in respect of passenger number, are *Shinjuku*, *Ikebukuro* and *Shibuya*: *Shinjuku* had 3.2 millions per a day as its number of passengers, *Ikebukuro* 2.6 millions, and *Shibuya* 2.3 millions, in 2006. This pattern does not coincide with the dominant mode.

We should overcome this discrepancy

First we introduce SPM Markov transition of Eq.4.1 to analyse the passenger distribution pattern. The initial condition of probability amplitude is a uniformly random distribution normalized by Euclidean norm. Fig.4.5 (a) depicts temporal variation of mode probability to reach dominant mode. The passenger distribution obtained is shown in Fig.4-5 (b), that corresponds to the authentic (political and business) centre of Tokyo: *Shinbashi*, *Shinagawa* and *Tokyo* are the dominant stations.

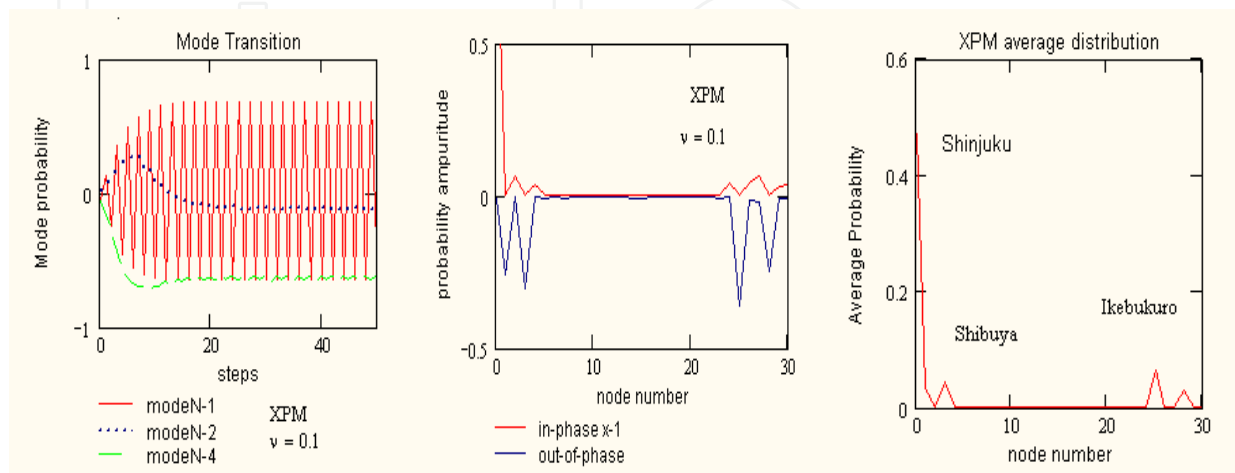


a) Temporal variation of mode amplitude

(b) The stationary state corresponds to the dominant mode.

Fig. 4.5. SPM Markov Transition of Tokyo Metropolitan Railway System.

Secondary, we introduce XPM Markov transition of Eq.4.2 to analyse the passenger distribution pattern. Fig.4.6 (a) depicts temporal variation of mode probability obtained for XPM. Mode #735 (N-1) having negative eigenvalue of -4.271 oscillates continuously and Mode #732 (N-4) having positive eigenvalue of $+4.423$ reaches to stationary state of -0.612 . This instability corresponds to sustainable commuting of random walkers between the two phases as shown in the middle panel of Fig.4.6.



Left: Temporal variation of mode amplitude, Middle: Two phase of oscillation. Right: Average Probability Distribution.

Fig. 4.6. XPM Markov transition of Tokyo Metropolitan Railway System

According to the discussion on the rosary network in subsection 4.1, the average observable state corresponds to three largest stations of Tokyo Metropolitan Railway system, as shown in the right panel of Fig.4.6. This pattern of passenger distribution might be recognized as a central zone of entertainments or young people's activity, comparing to the authentic centre of Tokyo discussed in SPM Markov transition.

These analyses suggest the importance of nonlinear interaction in passenger distribution of railway network systems. This non-linearity of passenger flow reflects a human nature such as "Birds with a feather flog together".

4.3 Network dynamics and Markov process

The most basic assumption of the nonlinear Markov transition is the synchronous transition among all of the nodes in the network. The probability amplitude of higher-order mode varies in sign at nodes so that the superposition in transition causes complicated interferences among various routes of transition.

These multiple path interference may cause oscillation and dominates dynamics of network system. The multiple path interference may have relation with chromatic number in local structure.

The possibility of sustainable oscillations, including relation of chromatic number, was reported in the ICCS (International Conference of Complex System) in Boston, July 2011. However, no experimental evidence is reported yet. (Ozeki, 2011)

5. “Tsubo” of network system

“Tsubo therapy” inspired us to study “Impulse response” in network dynamics: The impulse response in electrical circuit theory provides “frequency response function”, through the Fourier Transform, that makes it possible to analyse various dynamics of the circuit system. We named “an impulse applied at a node” as “point stimulus”, after professor H. Horiike, architect: winner of Grand Prix of the Dedalo-Minosse International Award’02, Italy. (Horiike, 2000); The point stimulus is expressed as the initial condition $-\delta(i, p)$ of the Markov transition, where $\delta(\cdot)$ is the kronecker delta, and p denotes the node where the impulse is applied. So far, this study is at dawn and a lot of unexplored remains. This section is based on our paper presented at KDIR2010 (International conference on Knowledge Discovery and Information Retrieval 2010).

5.1 Point stimulus response of Tokyo metropolitan railway system

Here we would like to show examples of point stimulus responses in Tokyo Metropolitan Railway System as illustrated in Fig.5.1: the upper row denotes those of “Shinjuku”, “Harajuku” and “Shibuya”. These point stimulus responses are dumping oscillations having fairly large amplitude of #735 mode. As discussed in subsection 4.2, since *Shinjuku* and *Shibuya* are the two of largest stations in Tokyo Metropolitan Railway System, and their degrees are sufficiently large, it is reasonable that they have larger point stimulus responses. On the contrary, “Harajuku” shows fairly large point stimulus response, but is a small station from viewpoint of its degree. The degree of *Harajuku* is only two compared to 11 of *Shinjuku*. In real world, “Harajuku” is a small station, but a famous down of youths and fashions. It can be said that the larger point stimulus response of “Harajuku” suggests that the point stimulus response is a reasonable tool to evaluate station activity.

The lower row denotes point stimulus responses of “Shinagawa”, “Yurakucho” and “Tokyo”. As discussed in subsection 4.2, those stations belong to the group of “authentic centre of Metropolitan Tokyo”. The dumping oscillations occur in eigenmode #734 that is the mode having negative second largest eigenvalue of -3.947. “Shinagawa” and “Tokyo” are fairly large station but the point stimulus responses are not so large that may reflect declining of those areas in 2006. Recently it can be said there are many successful projects to refresh these areas, such as *Shinagawa* intercity project. On the contrary, *Yurakucho* shows a relatively larger point stimulus response compared to small degree of 4. It can be said that the point stimulus response well reflects the town activity of *Yurakucho*.

Fig.5.2 denotes the cases that point stimulus responses reflect the miscellaneous station activities. The cases of “Akihabara” with degree of 7, “Meguro” with degree of 4 and “Otsuka” with degree of 2 are illustrated.: The point stimulus response well reflects the declining activity of “Akihabara” in spite of various projects for activation. “Meguro” and “Otsuka” seem to have larger point stimulus responses than their actual activities. It requires further studies whether these discrepancies suggest the chance of investments for town activation or not. We demonstrate the point stimulus response as one of interesting tool of checking the activity of node. It is expected that the point stimulus response is a clue to find the real affects of networking on a node.

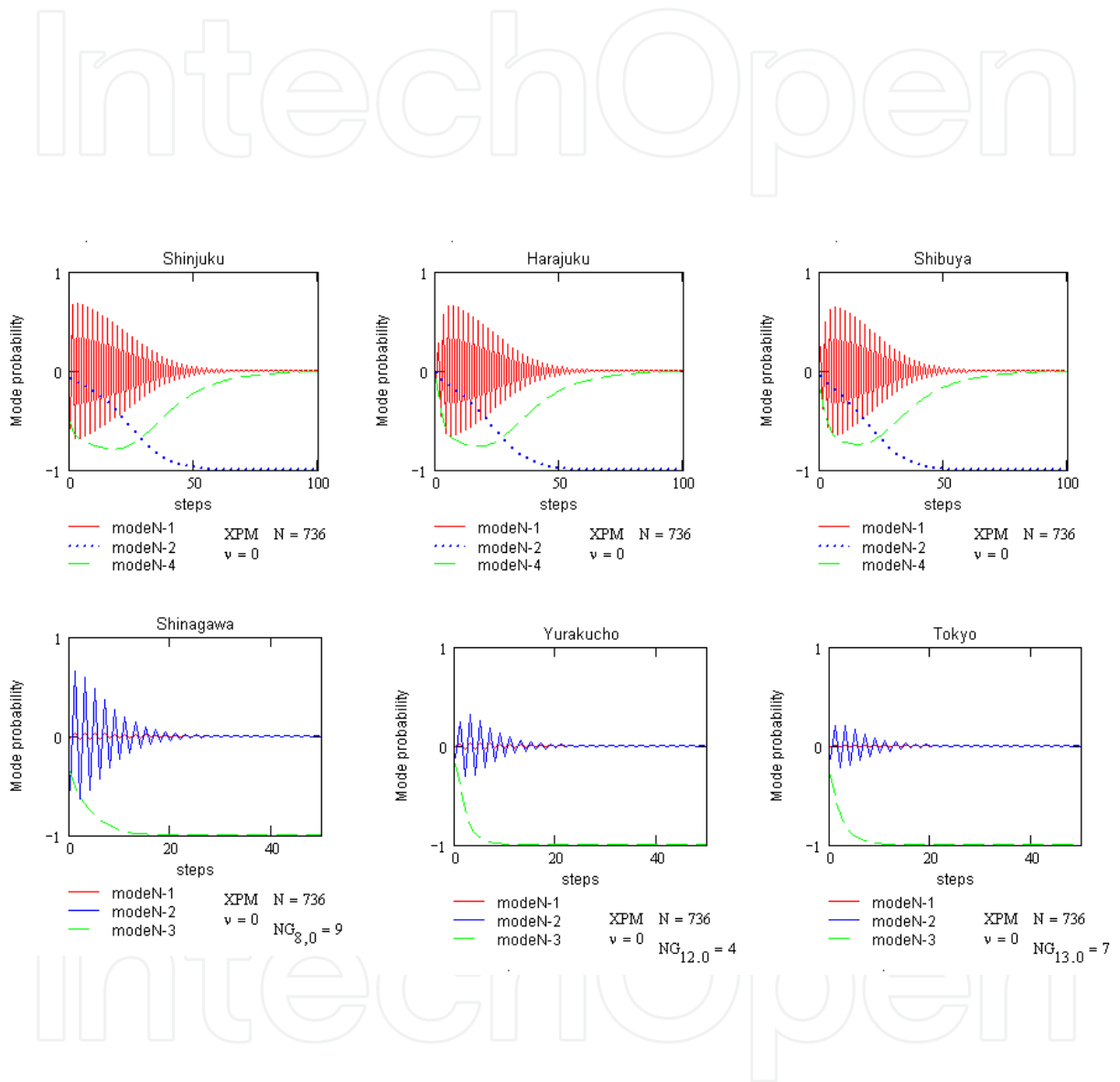


Fig. 5.1. Reasonable correlations of “point stimulus responses” with station activities.

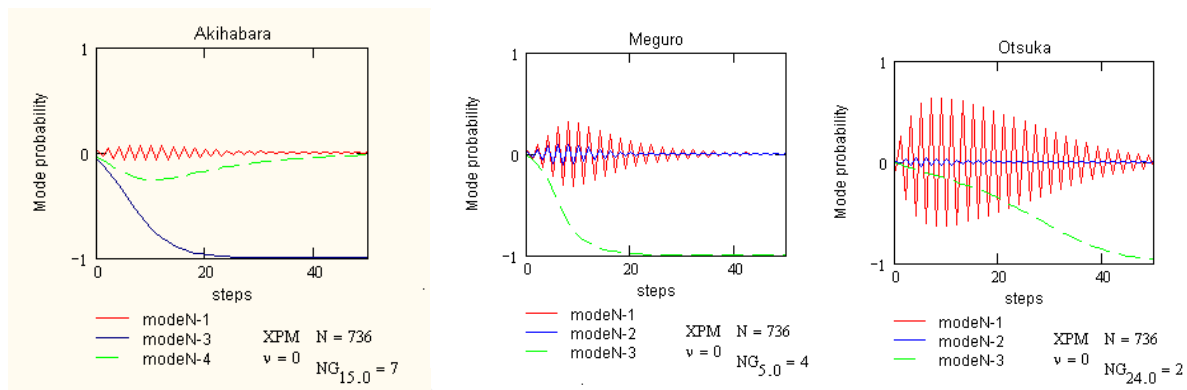


Fig. 5.2. Miscellaneous “point stimulus response”

6. Conclusion

We demonstrate a new network analysis based only on network topology of Tokyo Metropolitan Railway System. It is highly abstract and seems like a metaphor without any rigorous physical approval. However, many of the analyses seem to illustrate the truth of the railway system from an abstract viewpoint.

Rene Descartes wished all of the world could be described mathematically, then, as his first step, analytical geometry was innovated. Prigogine, the originator of complex systems, declared a “new alliance” between natural sciences and human sciences to solve global issues of human beings.

Here, we report a tiny effort of topological analysis of railway systems in this context. It is our wish to explore the horizon of our new mathematical platform as a tool for supporting the intuitive power of railway system designers.

The multimodal analysis based non-linear Markov transition approximation is still in its dawn. There are vast amounts of works unexplored for the future.

7. Appendix 1 – Mathematical platform

This section is based on our paper presented in ICCS (International Conference on Complex Systems) 2011.

7.1 A new rule introduced in mathematical platform

After the complex systems were originated by Ilya Prigogine from various foundations including irreversibility and self-organization in nonlinear dynamics (Prigogine, 1996), Barabasi introduced scale-free networks for describing interaction between structures or constituents of complex network systems (Barabasi 2002). On the other hand, Brin and Page simulated a web surfer by Markov transition through network linking web pages (Brin, 1998). Then they found with their surprise, in spite of personal inference of the Page Rank, that the web-network graph can rank the page importance mechanically by its dominant eigenvector (Brin, 1998, Langville 2006). We were inspired from these historical flows to construct a multi-modal platform of Markov transition with nonlinear interaction for analysing complex networks.

A new rule of Euclidian norm, introduced in normalization in Markov transition approximation, provides us a new multi-modal description of complex systems: The Markov transition approximation of Page-Ranking in Google uses only the dominant mode, because their elements of the eigenvector are positive semi-definitive, and so, can be recognized as the probability finding a web surfer on a web page.

However, the elements of the eigenvectors of higher order modes are not positive semi-definitive, so that a new rule is necessary for defining the probability to find the web surfer on the page in higher order mode. It is well known that, in the power method for analysing eigenmode of such an adjacency matrix, the state vector at each transition is normalized by its Euclidian norm to prevent divergence. Since the sum of squared elements of the state vector is normalized to unity, the squared elements of the state vector can be recognized as the probability finding the web surfer on each node, just analogous to the quantum physics. In this way, we can describe the multi-modal behaviours of complex network systems employing the nonlinear Markov transition approximation (Ozeki, 2009).

7.2 Topology dependent characteristics of various networks

For analysing topology dependent characteristics, it is necessary to generate scale free networks having different topological characteristics, as references. Here we employ the Granvetter's family network series [Ozeki2006:]. Using family network series, various topology dependent characteristics of scale free networks can be reviewed, in terms of chromatic number, degree correlation, clustering coefficient, and network entropy. Among these reviews, we report a sustainable oscillation caused by the unique eigenmode structure of BA-network. This topology dependent instability, which arises from mode competition in a special mode structure, named "skew degenerate modes", is observed in the most popular BA networks (Barabasi, 2002). The skew mode is discussed more in A.3.

7.3 A mathematical platform of network multimodal analysis

Now we summarize a mathematical platform for network analysis in multi-modal scheme. The platform is based on the Markov transition to approximate the variation of network state: A symmetric adjacency matrix, providing an orthogonal eigenvector set, is suitable for multi-modal analysis of a network system. However, divergence in the Markov transition using the adjacency matrix as the transition matrix is a serious problem. Here, we apply a mathematical procedure, being used in "the power method" (Langville, 2006), for preventing the divergence: In Markov process approximation, the variation of network state given by

$$\hat{q}_{n+1} = A \cdot \hat{q}_n \quad (\text{A1})$$

is described explicitly in the power method by

$$\hat{q}_{n+1} = A \cdot \hat{q}_n / \|A \cdot \hat{q}_n\| \quad (\text{A2}),$$

where \hat{q}_n is the state vector at the n^{th} transition step. The state vector is normalized with respect to the Euclidean norm $\|A \cdot \hat{q}_n\|$ after each transition step. This mathematical idea used in the power method assures the stability and also assures the linear properties of the Markov transition.

Furthermore, this idea lead us to read the state vector $(q_i)_n$ as a probability amplitude. The probability is defined by $(p_i)_n = |(q_i)_n|^2$ for finding a random walker at the node “ i ”, because the sum of probability $(p_i)_n$ over all nodes is normalized to unity as shown in Eq.A2.

The eigen-equation is $A \cdot \phi_i^{(m)} = \lambda_m \cdot \phi_i^{(m)}$ where λ_m is the eigenvalue of mode “ m ”, and $\phi_i^{(m)}$ is its eigenvector. The eigenvectors can be coincident with the asymptotic solution of Eq.A2 in the power method.

7.4 Markov transition with weak non-linearity

It is essential for the network analysis platform to be capable to analyse nonlinear phenomena. We introduce a non-linear Markov transition as follows: the nonlinear interaction in Markov transition means that transition from node “ j ” to node “ i ” is affected by the probability amplitude $(q_k)_n$ at node “ k ” linked to the node i , that is

$$(q_i)_{n+1} = \sum_j A_{i,j} \cdot (q_j)_n + \sum_{j,k} \nu \cdot A_{j,i} \cdot A_{k,i} (q_j)_n \cdot (q_k)_n \quad (\text{A3})$$

where ν is a measure of nonlinear interaction. Eq.A.3 includes implicitly the normalization process as shown in EqA.2. This expression agrees with the definition of the Markov process, that is, the transition is determined only by the states at the present step n . The 3rd order nonlinear Markov transition is introduced in section 4.

8. Appendix 2 – Variety of topological parameters in family networks

The family network series, visualized in Table A1, provides variety of topological parameters of networks, such as degree correlations, clustering coefficients, and network entropies. These parameters are plotted in Fig.A.1 to understand details. The red line in the figure denotes a typical variation of the degree Pearson correlations depending on the constituent family size M of family network series. A “typical variation” means that the degree correlations shown in Fig.A.1 is the mean value of those calculated for 10 samples of networks, having about 100 total nodes, for each. The BA network is known as a disassortative network, that is, nodes with low degrees are more likely to be connected to the nodes with high degrees, and vice versa. The family networks with larger size M of constituent family become to be assortative, that is, nodes with a given degree are more likely to have links with nodes of similar degree. These Pearson coefficients of degree correlation (Soramaki, 2007) are illustrated in Fig.A.1 as a red line.

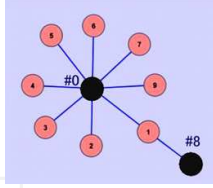
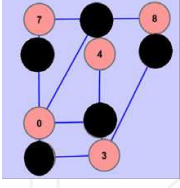
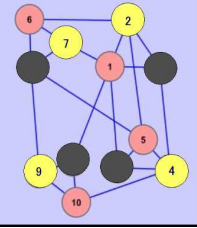
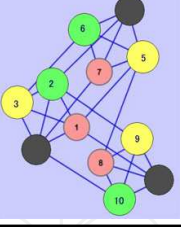
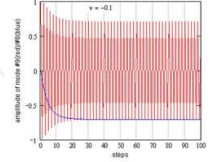
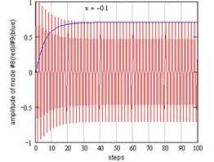
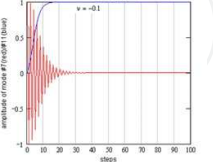
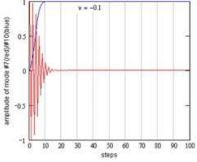




Family Network Topology (ref. ICCS2006,id405)				
Temporal Response (Non-linear Markov)				
Chromatic Number	 2	 2 or 3	 More than 3	 More than 4
Entropy	1.0	1.9	2.0	2.0
Degree Correlation	-0.30	-0.10	0.11	0.15
Clustering Coefficient	0	0	0.24	0.37
Asymptotic Exponent	3	4	5	6

Table A.1. Topology Dependent Network Dynamics

A clustering coefficient of a node is defined by the ratio of the actual number of links among neighbours of the node over the number of potential links among them. The clustering coefficient of the network is the mean clustering coefficient over all of nodes. The blue line in Fig.A.1 denotes the clustering coefficients of family networks. The family network with larger M has higher clustering coefficient.

Three kinds of entropy can be defined in multimodal description:

The first one is the node entropy NE_i that is defined by the sum of Shannon entropies over all of modes, that is,

$$NE_i = -\sum_m p_i^{(m)} \ln p_i^{(m)}. \quad (A4)$$

The second is the mode entropy ME_m that is defined by the sum of Shannon entropies over all of nodes, that is,

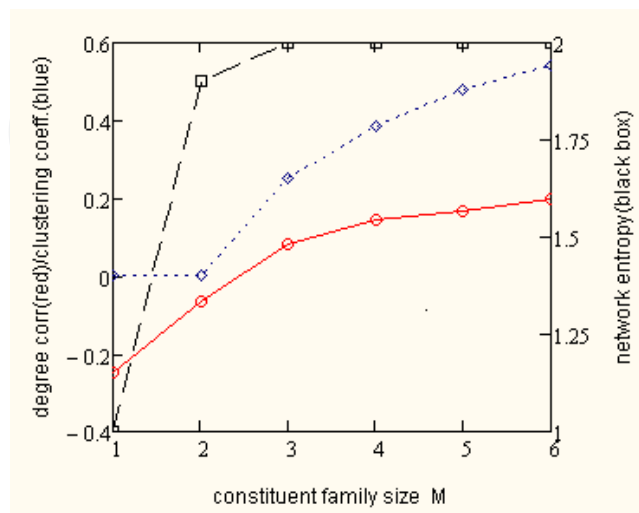
$$ME_m = -\sum_i p_i^{(m)} \ln p_i^{(m)}. \quad (A5)$$

The third is the network entropy that is defined by the sum of node (or mode) entropies over all of nodes (or modes), that is,

$$NetE = \sum_i NE_i = \sum_m ME_m. \quad (A6)$$

The network entropy is plotted by black line with diamonds in Fig.A.1, corresponding the family network shown in Table A1.

The variety of topological parameters of the family network provides a possibility of better approximation for a given network topology: We can approximate a network topology generated by the family network growth mechanism, with selecting the size M of constituent family randomly at the entry to meet its statistics, such as size of household (Ozeki, 2009).



Red line denotes the degree correlation using Pearson's formula and Blue dotted line denotes the clustering coefficient. Black line with diamonds denotes the network entropy with the right-hand scale.

Fig. A.1.1. Topological parameter variation of family network series

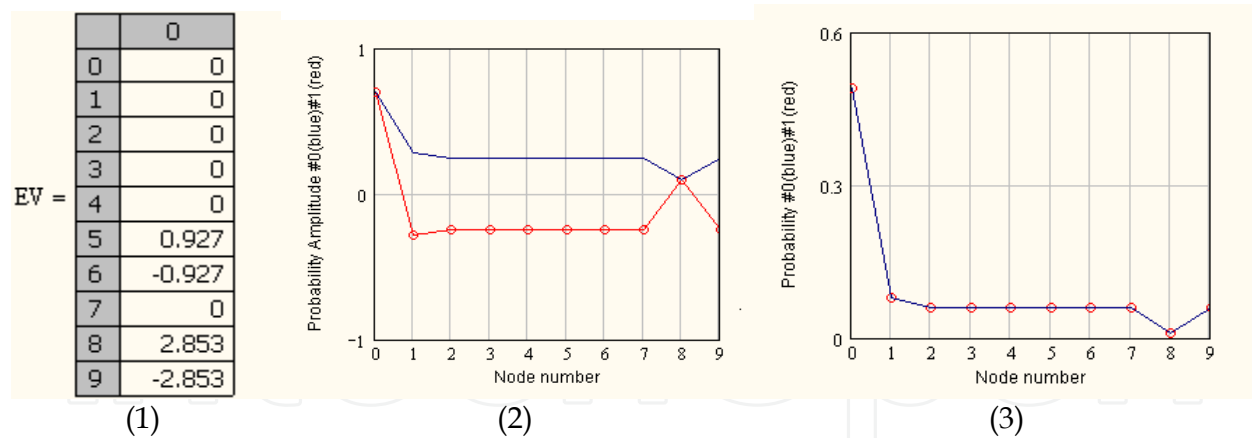
9. Appendix 3 – Skew degeneracy

In Table A1, family network series are illustrated with the smallest number of colours: the chromatic number of a graph, in the third row in Table A1, is the smallest number of colours such that no two adjacent nodes share the same colour (<http://mathworld.wolfram.com/chromaticNumber.html>). This chromatic number is strongly related to the symmetry of the graph.

The BA network has the same chromatic number as the coupled harmonic oscillators, which consist of a long chain of masses and springs. Dyson analysed the coupled oscillators in 1953 to find mode pairs having the same eigenvalue in absolute value but different in sign (Dyson, 1953).

Degeneracy generally refers to objects having the same eigenvalue but different in eigenvectors, whereas the skew degeneracy, we named, refers to objects having different eigenvalues with respect to the sign of the eigenvalue but having the same probability distribution, that is the square of the eigenvectors normalized with respect to the Euclidean norm.

For an example, Fig.A.3.1 (1) shows the eigenvalue of the adjacency matrix of the BA network $M=1$ illustrated in Table A1, that includes two pairs of skew degeneracy modes. Fig.A.3.1 (2) illustrates the eigenvectors corresponding to a skew degenerate mode pair: Blue line denotes the dominant mode #8 having eigenvalue of +2.853, and Red line with circles denotes the mode amplitude of mode #9 having eigenvalue of -2.853. Fig.A.3.1. (3) denotes their probability distributions of mode #8 and #9 that coincides with each other.



(1)Eigenvalue (2) Mode amplitudes: Blue line denotes the dominant mode (#8) having eigenvalue of 2.853 Red line with circles denotes the mode amplitude of mode #9 having eigenvalue of -2.853
(3)Probability Distribution :Both of skew modes coincide.

Fig. A.3.1. Skew Degenerate Mode Pair of BA network (M=1)

The family network with M=2 has a possibility having mode pairs of skew degeneracy. However, the other family networks with larger M than 3 do not show the skew degeneracy.

9.1 Temporal response of skew degenerate modes in nonlinear Markov transition

The nonlinear Markov transition of Eq.A.3 can be converted to the description of the nonlinear interaction of mode amplitudes for getting clearer image, as the following:

$$(a_m)_{n+1} = \lambda_m \cdot (a_m)_n + \sum_{i,m',m''} v \cdot \lambda_{m'} \cdot \lambda_{m''} \cdot \phi_i^{m'} \cdot \phi_i^{m''} \cdot \phi_i^m \cdot (a_{m'})_n \cdot (a_{m''})_n \quad (A7),$$

where the modes are defined by the linear adjacency matrix. It should be noted that the equivalency of Eq.A.3 and Eq.A.4 is limited only for the case of very weak non-linearity considered.

The transient response of the network having the skew degeneracy shows the sustainable oscillation in the nonlinear Markov transition as shown in the second row of Table A.1. The initial conditions are the modes with the negative largest eigenvalue. The skew mode pair survives in mode competition so that the random walker continues to commute between two states that are the superposed states of the skew degenerate modes with in-phase and out-of-phase, respectively. The two states correspond to the group of the black and the red nodes in the BA -network, so that the random walker commutes between the node groups of red and black.

Fig.A.3.2 illustrates these situations clearly; the probability amplitude distribution is given by $(q_i)_n = \sum_m (a_m)_n \cdot \phi_i^{(m)}$, that corresponds to the superposition of two competing modes #8 and #9 illustrated in Fig.A.3.2 (2): The mode amplitude $(a_9)_n$ in red of Fig.A.3.2 (1) continues to oscillate between $+1/\sqrt{2}$ and $-1/\sqrt{2}$ whereas $(a_8)_n$ in blue grows up to $-1/\sqrt{2}$ so that the superposition of two competing modes corresponds to red line of in-phase and blue line of out-of-phase as shown in Fig.A.3.2 (2).

The node patterns illustrated by red and blue lines coincide with the chromatic groups shown in the first row of Table A.1.

On the other hand, the family networks with $M \geq 3$ show quicker transition to the stationary state corresponding to the dominant mode, as shown in the second row of Table A.1.

It is shown the following; the topology dependent instability dominates the temporal response in controlling the network system so that the network topology determines the dependability of the system, in a sense.

10. Appendix 4 – Family network series as reference

10.1 Network growth mechanism of family network

The session 2 of reference(Ozeki, 2006) should be read as follows: The asymptotic connectivity distributions of the full-mesh family networks are derived by the method reported by Dorogovtsev et al. At initial time $t=1$, the number of constituent family is one so that the number of nodes is M . We assume the node attractiveness is given by $A+M-1$ where the number of links is $M-1$, so that the total attractiveness is $M(A+M-1)$. At time $t=t$, the total attractiveness of the network is $M(A+M-1)t+M(t-1)$, where the last term $M(t-1)$ is the contribution of the weak ties. By replacing these in equations $p(k,s,t+1)$, then the connectivity distribution $p(k)$ is given by

$$p(k) = \frac{1}{2} \frac{\Gamma(2M+2A+1)}{\Gamma(M+A)} \frac{\Gamma(k+A)}{\Gamma(k+M+2A+1)} \quad (\text{A10})$$

We obtain the asymptotic exponent $\gamma = M + 1 + A$.

10.2 Network stabilization by topological improvement

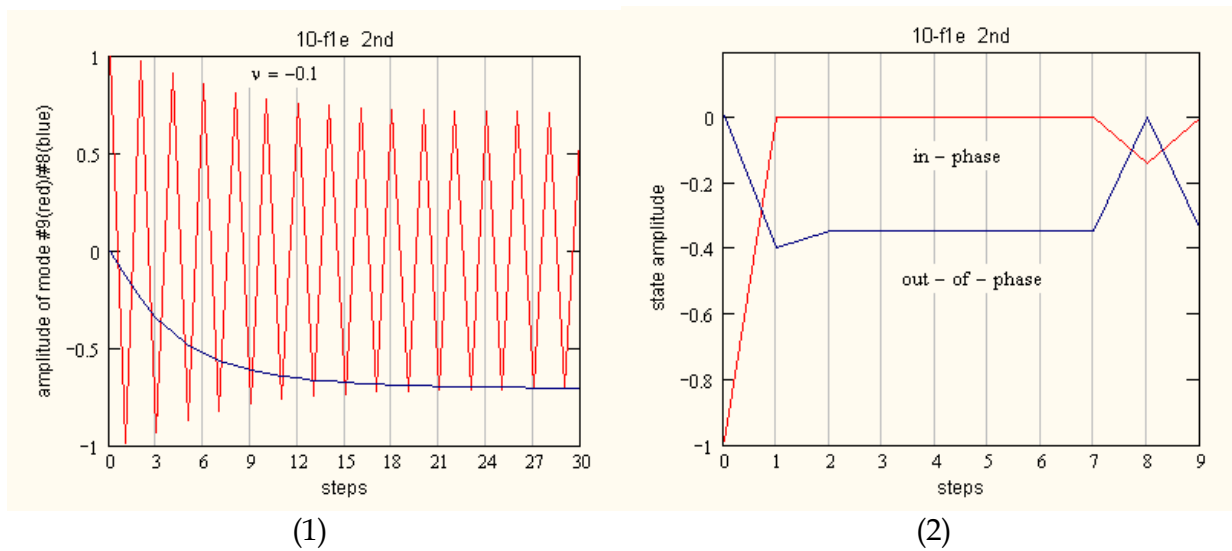
The network dynamics such as stability of the network system depends on the topology of the network system. Family network series gives us typical dynamics variations, as shown in TableA.1, as a reference. These understanding seem helpful to design network such as railway system.

So far there is no experimental evidence showing these transient behaviours of networks yet, but we can imagine several examples intuitively as follow:

a BA network with 100 nodes is illustrated in Fig.A.4.1 (1). The node # 0, and #1 and #2 are larger hubs. We might assume it as an ancestry of a family struggle, or an organization map just after consolidation of three small consanguineous companies. This topology consists of 26 pairs of skew degenerate modes and shows sustainable oscillation from an initial condition of random probability amplitude distribution as shown in Fig.A.4.1 (2). This might correspond to longer periods of struggles or troubles in this network system.

An intuitive method to prevent these troubles is to span a new link between two hubs, node #1 and #2 as shown in Fig.A.4.1 (3). This method is confirmed to be effective to convert the sustainable oscillation to quicker transition to stable state, by the non-linear Markov transition simulation, as shown in Fig.A.4.1 (4).

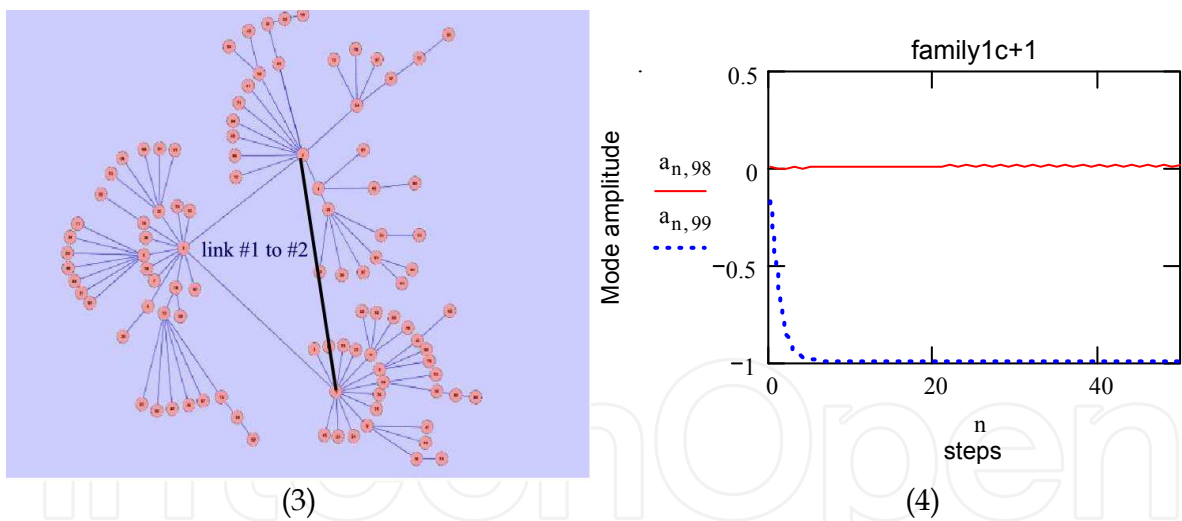
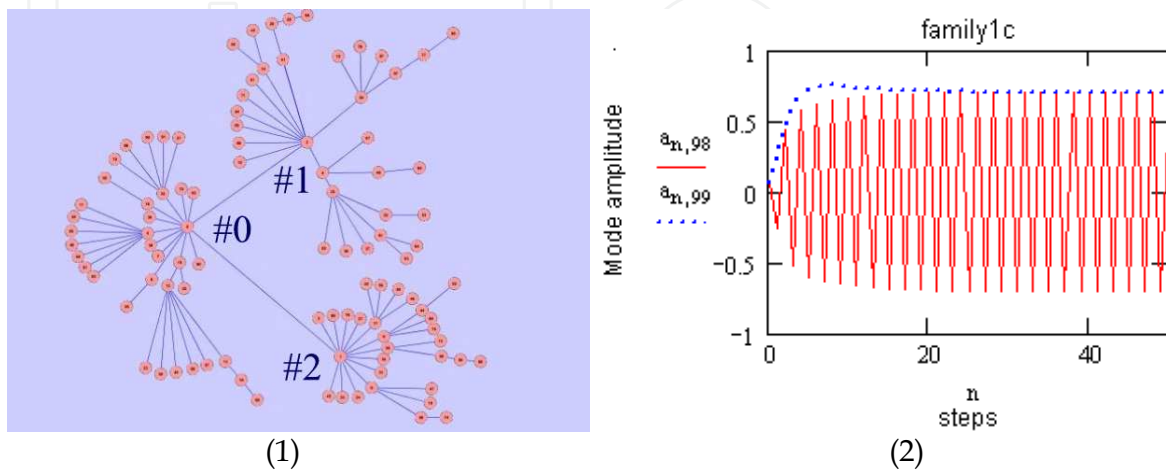
IntechOpen



(1) mode amplitude $(a_9)_n$ in red and $(a_8)_n$ in blue, (2) the state amplitude of superposition.

IntechOpen

Fig. A.3.3. In-Phase and Out-of-Phase Superposition of Skew Degenerate Mode Pair

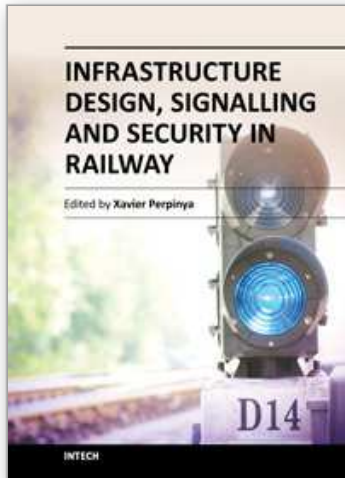


(1) BA network with 100 nodes, (2) Sustainable oscillation of skew degenerate mode pair, (3) Topological improvement by connecting #1 and #2, (4) The topological improvement can convert the sustainable oscillation to quicker transition to stable state.

Fig. A.4.1. Topological Improvement of Network System Stability

11. References

- Agrawal, G.P., (1989) "Nonlinear Fiber Optics", Academic Press, San Diego.
- Barabasi, A. L., Albert, R. and Jeong, H. (1999) "Mean field theory of scale free random networks", *Physica A*, 272, 173.
- Barabasi, A. L. and Albert, R. (2002) "Emergence of scaling in random networks", *Science* 286, 509.
- Barabasi, A. L., (2002) "Linked", Penguin Group, New York
- Buchanan, M. (2002) "Nexus", W.W. Norton & Company Ltd., New York.
- Brin, S. and Page, L. (1998) "The anatomy of a large-scale hypertextual Web search engine", *Computer Networks and ISDN Systems*, 33:107-17, 1998
- Erdos, P. and Renyi, A. (1960) *Publ. Math. Inst. Acad. Sci.* 5, 17.
- Dorogovtsev, S. N, Mendes J F and Samukhin, A. N. (2000) "Structure of growing networks with preferential linking". *Phys. Rev. Lett.* 85, 4633-4636 (2000).
- Dyson, F.J. (1953) "The Dynamics of a Disordered Linear Chain.", *Phys. Rev.* Vol. 92, No. 6, 1331.
- Haken, H. (1978) "Synergetics, An Introduction. Nonequilibrium Phase Transitions and Self-Organization in Physics, Chemistry and Biology", Springer, Berlin.
- Horiike, H. (2000), private communication.
- Granovetter, M. (1973) "The strength of weak ties.", *American Journal of Sociology*, 78, 1360-1380.
- Langville, A and Mayer, C, (2006) "Google's PageRank and Beyond". Princeton University Press, Princeton and Oxford.
- Newman, M., Barabasi, A.L. and Watts, J. (2006) "The structure and Dynamics of Networks" Princeton Univ. Press.
- Ozeki, T., and Kudo, T., (2009) Invited paper, IEICE Technical Report, "A Proposal of Network Evaluation Method and Its Applications" vol. 109, no. 220, IN2009-65, PN2009-24, pp 13-21.
- Ozeki, T. (2006) <http://necsi.org/events/iccs6/viewpaper.php?id=405> We found a mistake in session 2 of our "Evolutional family networks generated by group-entry growth mechanism with preferential attachment and their features.", The International Conference on Complex Systems, id 405, Boston. The asymptotic exponent should be read as $M+A+1$
- Ozeki, T. (2010), "Multimodal Analysis of Complex Network-Point stimulus response depending on its location in the network-" Knowledge Discovery and Information Retrieval 2010, Valencia, Spain, 2010.
- Prigogine, I. (1996) "The end of certainty", The Free Press, London
- Soramaki, K, Bech, M L, Arnold, J, Glass, R J and Beyeler, W E, (2007) "The topology of interbank payment flows", *Physica A: Statistical Mechanics and its Applications* Vol 379, Issue 1, June 2007, pp 317-333.
- Tsuji, S. (1983), "Transmission Circuits", Colona Publication Inc. Tokyo.
- Watts, D. J. and Strogatz, S. H. (1998), "Collective dynamics of "small-world" Networks", *Nature* 393, 440-442.



Infrastructure Design, Signalling and Security in Railway

Edited by Dr. Xavier Perpinya

ISBN 978-953-51-0448-3

Hard cover, 522 pages

Publisher InTech

Published online 04, April, 2012

Published in print edition April, 2012

Railway transportation has become one of the main technological advances of our society. Since the first railway used to carry coal from a mine in Shropshire (England, 1600), a lot of efforts have been made to improve this transportation concept. One of its milestones was the invention and development of the steam locomotive, but commercial rail travels became practical two hundred years later. From these first attempts, railway infrastructures, signalling and security have evolved and become more complex than those performed in its earlier stages. This book will provide readers a comprehensive technical guide, covering these topics and presenting a brief overview of selected railway systems in the world. The objective of the book is to serve as a valuable reference for students, educators, scientists, faculty members, researchers, and engineers.

How to reference

In order to correctly reference this scholarly work, feel free to copy and paste the following:

Takeshi Ozeki (2012). Topological Analysis of Tokyo Metropolitan Railway System, Infrastructure Design, Signalling and Security in Railway, Dr. Xavier Perpinya (Ed.), ISBN: 978-953-51-0448-3, InTech, Available from: <http://www.intechopen.com/books/infrastructure-design-signalling-and-security-in-railway/topological-analysis-of-tokyo-metropolitan-railway-system>

INTECH
open science | open minds

InTech Europe

University Campus STeP Ri
Slavka Krautzeka 83/A
51000 Rijeka, Croatia
Phone: +385 (51) 770 447
Fax: +385 (51) 686 166
www.intechopen.com

InTech China

Unit 405, Office Block, Hotel Equatorial Shanghai
No.65, Yan An Road (West), Shanghai, 200040, China
中国上海市延安西路65号上海国际贵都大饭店办公楼405单元
Phone: +86-21-62489820
Fax: +86-21-62489821

© 2012 The Author(s). Licensee IntechOpen. This is an open access article distributed under the terms of the [Creative Commons Attribution 3.0 License](#), which permits unrestricted use, distribution, and reproduction in any medium, provided the original work is properly cited.

IntechOpen

IntechOpen